Research article; VSI: genomic palaeoecology

# Diversification and historical biogeography of the Himalayan toad (*Duttaphrynus himalayanus*)

Sylvia Hofmann[a,b,†], Dennis Rödder[a], Joachim Schmidt[c], Morris Flecks[a], Daniel Jablonski[d], Alain Dubois[e], Annemarie Ohler[e], Chitra, B. Baniya[f], Vladimir Vershinin[g,h], Spartak N. Litvinchuk[i], Christophe Dufresnes[e,†]

[a] *Museum Koenig, Leibniz Institute for the Analysis of Biodiversity Change, Adenauerallee 127, 53113 Bonn, Germany;* s.hofmann@leibniz-lib.de, d.roedder@leibniz-lib.de, m.flecks@leibniz-lib.de

[b] *Helmholtz-Centre for Environmental Research – UFZ, Permoserstrasse 15, 04318 Leipzig*

[c] *General and Systematic Zoology, Institute of Biosciences, University of Rostock, 18055 Rostock, Germany;* agonumschmidt@hotmail.com

[d] *Comenius University in Bratislava, Ilkovičova 6, Mlynská dolina, 842 15, Brastislava, Slovakia;* daniel.jablonski@uniba.sk

[e] *Institut de Systématique, Evolution, Biodiversité (ISYEB), Muséum national d'Histoire naturelle, CNRS, Sorbonne Université, EPHE-PSL,Université des Antilles, 55 rue Buffon, CP 51, 75005, Paris 75005, France;* alain.dubois@mnhn.fr; annemarie.ohler@mnhn.fr; christophe.dufresnes@mnhn.fr

[f] *Central Department of Botany, Tribhuvan University, Kirtipur 44618, Kathmandu, Nepal* cbbaniya@gmail.com

[g] *Institute of Plant and Animal Ecology, Ural Branch of the Russian Academy of Sciences, Yekaterinburg, Russia*

[h] *Institute of Natural Sciences and Mathematics, Eltsyn Ural Federal University, Yekaterinburg, Russia* vol_de_mar@list.ru

[i] *Institute of Cytology of the Russian Academy of Sciences, St. Peterburg, Russia, 194064* litvinchukspartak@yandex.ru

† Corresponding authors: s.hofmann@leibniz-lib.de, christophe.dufresnes@mnhn.fr

**Abstract**

The Himalaya harbors a unique faunal diversity shaped by major geological events and the resulting paleoenvironmental changes. Retracing the evolution of Himalayan species thus offers a window to understand how mountain formation and climatic shifts influenced their diversification. Using genomic analyses and paleoclimatic species distribution modeling, we reconstructed the evolutionary history of the Himalayan toad (*Duttaphrynus himalayanus*), a montane amphibian widely distributed across the Himalayan range. Our analyses reveal two major phylogeographic lineages in *D. himalayanus*—east and west of the Thakkhola basin (upper Kali Gandaki River)—that diverged during the Late Pliocene (~3.2 Mya) and seemingly show traces of recent gene flow. Patterns of divergence in the eastern lineage suggests additional phylogeographic structure between Nepalese and Bhutan ranges in the central Himalaya. The two lineages show differences in climatic space (especially precipitation), but not necessarily ecological divergence, suggesting that topographic barriers are a primary factor of differentiation. Our results suggest that *D. himalayanus* is a relatively young montane lineage compared to other Himalayan amphibians that diversified within the uplifted Himalaya rather than originating from paleo-Tibetan or Indochinese ancestors. The resulting hidden diversity seems primarily shaped by topographic barriers, notably the Kali Gandaki, despite episodic connectivity that was possibly facilitated by paleolake corridors formed during the Late Quaternary. These findings imply that taxonomic revisions in *D. himalayanus* are required, and call to further similar studies in other Himalayan herpetofauna to identify common drivers of biogeographic diversification across these mountain environments.

**Key words**: Bufonidae, ddRAD-sequencing, Himalaya, Kali Gandaki, Thakkhola Basin

## 1. Introduction

The Himalaya, together with the Tibetan Plateau, forms the largest and highest mountain system on Earth, exerting a profound influence on global climate and the biodiversity of Asia. The southern slopes of the Himalayan range are recognized as a biodiversity hotspot (Mittermeier et al., 2004; Mittermeier et al., 2011), hosting a unique assemblage of plant and animal species shaped by the dynamic geological history and shifting paleoclimates of the Himalayan-Tibetan orogen (HTO).

Recent years have seen significant revisions to geoscientific models of the HTO's formation, although these models remain a topic of ongoing debate. Earlier theories proposed a highly elevated Tibetan Plateau with alpine habitats as far back as the Eocene or even earlier (Kapp et al., 2007; Murphy et al., 1997; Rowley and Currie, 2006; Tapponnier et al., 2001; Wang et al., 2014; Xu et al., 2013). In contrast, modern concepts, incorporating fossil evidence and revised paleoelevations, suggest a subtropical to warm-temperate paleoclimate across large parts of the present-day plateau during this time (Pan et al., 2024; Spicer et al., 2021a; Spicer et al., 2021b). Simultaneously, recent advances in phylogenetic studies of Himalayan taxa (ground beetles, amphibians) of the cloud forest fauna suggest that southern Paleo-Tibet may have served as an important evolutionary center during the Cenozoic. Climate changes driven by ongoing uplift of the HTO likely reshaped environmental niches, prompting species to shift their ranges into the emerging Himalaya during the Miocene, as their ancestral habitats in Paleo-Tibet disappeared (Hofmann et al., 2024a; Hofmann et al., 2024b; Schmidt et al., 2012). This scenario challenges the widely held assumption that the Himalaya was predominantly colonized by species expanding westward from Indochina, or vice versa, migrating parallel to the growing Himalayan Mountain range (Ahrens, 2004; Martens, 1993; Wambulwa et al., 2021; Xing and Ree, 2017). In montane, less migratory taxa of early to mid-Miocene origin, the east-to-west or west-to-east dispersal model may not adequately explain their present-day distribution patterns and phylogenetic structure (Hofmann et al., 2024b; Hofmann et al., 2017).

For Himalayan species that emerged during the Late Miocene or perhaps not until the Pliocene – likely coinciding with the later stages of the HTO formation – their historical biogeography is likewise primarily characterized by immigration scenarios (see above), particularly for highly mobile species, such as plants (Cun and Wang, 2010; Liu et al., 2018), birds (Johansson et al., 2007), and

butterflies (Mani, 1986). In contrast, the evolutionary patterns of other groups with limited dispersal abilities and low vagility remain poorly understood. The uplift of the Himalaya not only created significant physical barriers to the north but also along its east-west axis, which likely restricted dispersal and gene flow. These geographic and ecological constraints are believed to have played a key role in fostering the region's exceptional levels of endemism and biodiversity (White, 2016). Understanding these processes is crucial for unraveling the evolutionary history of Himalayan biota and could provide broader insights into how geological and climatic changes have shaped species distributions and diversification during the final stages of the HTO's evolution.

The Himalayan toad *Duttaphrynus himalayanus* (Günther, 1864), a member of the true toad family (Bufonidae Gray, 1825), is widely distributed at the southern slopes of the Himalaya (Fig. 1). Bufonids likely originated in the New World and are thought to have reached Eurasia either via the Thule or De Geer land bridges (Litvinchuk, 2011), or by dispersing first into Africa (Wu et al., 2025). From Eurasia, they rapidly expanded southward, eventually spreading to Africa, Southeast Asia, and the Indian subcontinent around the transition between the Oligocene and Miocene (Van Bocxlaer et al., 2009). Alternatively, if they entered Africa first, bufonids may have spread into Asia during the late Oligocene, and subsequently into Europe during the Miocene and Pliocene (Wu et al., 2025).

The Himalayan toad occurs in montane and high montane regions of the southern slope of the Himalaya, spanning northern Pakistan, northern India, southwestern China (Xizang), Nepal, and Bhutan (Fei et al., 2012). There are dubious reports of *D. himalayanus* from northwestern Yunnan, China, which are likely misidentifications of *D. stuartii*; so far, no verified occurrences or voucher specimens of *D. himalayanus* have been documented from this area. Above approximately 2,000 m a.s.l., it replaces its submontane/lowland sister species, *D. melanostictus*, a highly vagile and commensal species adapted to a wide range of habitats and with an origin in Southeast Asian mainland (Othman et al., 2020; Wogan et al., 2016). Recent studies indicate, that *D. himalayanus* represent a species complex, with at least two deeply diverged mtDNA lineages in eastern and western ranges (Kathiwada et al., 2021) that were dated to the Pliocene (4.1 Mya) (Dufresnes et al., 2025). Given its age, which aligns closely with the later stages of the HTO's evolution and considering the typically limited dispersal ability and low vagility of amphibians, this species serves as an ideal yet

understudied model for investigating how species colonized and adapted to the Himalayan mountains during the late Neogene. Considering this, and accounting the limit of mtDNA for amphibian phylogeography, we here explore the diversification and biogeography of *D. himalayanus* by carrying out analyses of genomic data obtained by double digest Restriction Associated DNA sequencing (ddRAD-seq) and species distribution modeling. Our sampling spans the central and western Himalaya, encompassing nearly the entire distribution range of the species.

## 2. Methods

### *2.1 Sampling*

A total of 33 ethanol-preserved samples of *Duttaphrynus himalayanus* and 5 of *D. melanostictus* [sensu stricto (Dufresnes et al., 2025); all from the sub-Himalayan region] were gathered for genetic analyses from museum specimens curated in herpetological collections, namely of the Muséum National d'Histoire Naturelle in Paris, France (MNHN), the Institute of Cytology of the Russian Academy of Science in St. Petersburg, Russia (INCRAS), the Comenius University in Bratislava (CU), the Natural History Museum in Erfurt, Germany (NME), the Museum Koenig, Bonn, Germany (ZFMK), and the Bavarian State Collection for Zoology, Munich, Germany (ZSM); few samples originate from live adults released after capture (Supplementary Material Table S1). For ddRAD-seq and mitochondrial sequencing, DNA was isolated from thigh muscles (vouchered specimens) or buccal swabs (live adults) using the Qiagen Blood & Tissue kit, following the manufacturer's protocol.

### *2.2 ddRAD-seq analyses*

A ddRAD-seq library was prepared following the protocol detailed previously (Dufresnes et al., 2025), which involves *MseI* and *SbfI* restriction enzymes and a fragment size selection range of 400–500 bp. The library multiplexed our 38 samples in a 92-samples pool (including samples from other projects) and was sequenced paired-end with the PE150 kit on a DNBSeq platform at BGI China, which yielded 460,941,035 reads. Raw reads were demultiplexed, de novo assembled and filtered for SNP calling in Stacks 2.60 (Catchen et al., 2013). Demultiplexing (*process_radtags*

function) included the removal of uncalled bases (–c), the filtering out of reads below a Phred quality score of 30 (–s 30), the rescue of barcodes and RAD tags (–r), the removal of adapter sequence (–adapter-1 and –adapter-2), allowing up to two mismatches (–adapter-mm 2), and the trimming of reads to 100 bp (–t 100). RAD loci construction, assembly and cataloging (*denovo_map.pl* pipeline) were processed with default values for –m, –n, and –M. The final catalog comprised 377,096 loci, with a mean effective per-sample coverage of 15.1×. SNP calling (*populations* function) involved adjusting the number of samples in each a locus must be present (–p) for the generation of supermatrix alignments (–phylip-var-all) and SNP matrices (–structure), subsequently converted and used in downstream phylogenetic and clustering analyses. Other parameters were left as default

Preliminary assessments revealed that two *D. himalayanus* historical samples from Bhutan showed few loci compared to the remaining samples. To avoid the issue of "bad apples" in ddRAD-seq analyses (Cerca et al., 2021) these important samples were analyzed separately.

From the main sample set (31 *D. himalayanus* + 5 *D. melanostictus* outgroup samples), three datasets were obtained and analyzed as followed.

First, we produced an alignment of 9,515 loci (1,529,563 bp) sequenced in at least 32 of the 36 samples (–p 32). This dataset was employed to perform a maximum-likelihood phylogenetic analysis with IQ-TREE 2 (Minh et al., 2020) using the model finder and a 1,000 bootstrap pseudo-replicate to assess branch support.

Second, for the 31 *D. himalayanus* samples, we produced a SNP matrix of 5,744 SNPs, each SNP being located on a different RAD locus (by randomly selecting one SNP per locus, –write-random-snp) and shared among all samples (–p 31), thus limiting physically linked SNPs and avoiding missing data. This was used to infer genetic clustering using the R package LEA (Frichot and François, 2015) testing 1 to 10 *K* groups, each with 20 replicates (10,000 iterations with the first 10 % as burnin), and computing cross-entropy estimates to evaluate the relevant number of clusters. A principal component analysis (PCA) on allele frequency was then performed with the R package *adegenet* (Jombart, 2008). Furthermore, we reported the observed heterozygosity of each sample computed by the *populations* function of Stacks. Custom R scripts were used for visualizing the results.

Third, to test for interspecific gene flow between *D. melanostictus* and *D. himalayanus*, we exported a matrix of 1,699 SNPs present in all 36 samples and representing different RAD loci (–p 36 –write-random-snp). A LEA clustering with K = 2 was performed to distinguish the two species and screen for individuals with shared ancestry.

The two low-read Bhutan samples were analyzed alongside nine samples representative of the *D. himalayanus* diversity identified in the main analyses (see Results), with an alignment and a SNP matrix of the locus present in all of them (–p 11). The alignment, consisting of 38 loci (5,959 bp) was analyzed with IQ-TREE2 as above, and the SNP matrix, consisting of 51 SNPs (retaining all loci given the low numbers of loci available), was again analyzed with LEA and by a PCA.

Finally, a time-calibrated species tree was constructed for a subset of 15 samples chosen to represent both sampled species and their corresponding phylogeographic lineages: two samples of *D. melanostictus*, 13 unadmixed samples from the two *D. himalayanus* lineages (see Results). To this end, we generated an alignment concatenating 6,942 RAD loci (1,124,532 bp) shared among all samples (–p 15). Phylogenetic reconstruction was performed using the SNAPP package within BEAST2 (Bryant et al., 2012). Input files were prepared using the Ruby script snapp_prep.rb (Stange et al., 2018) which allows time calibration of the species tree estimated by SNAPP through age constraints on divergence events, which facilitates time calibration of species trees estimated by SNAPP through the application of divergence time constraints. In the absence of fossil calibrations, we applied normally distributed MRCA priors (mean = 10.2 Mya, $\sigma = 1.8$) on the divergence between *D. melanostictus* and *D. himalayanus*, following a previous study (Dufresnes et al., 2025). Two independent SNAPP analyses were run, each with 10 million MCMC iterations. Chain convergence and stationarity were assessed visually using TRACER v1.6 (ESS > 1000; http://beast.bio.ed.ac.uk/tracer/). Posterior distributions of trees were visualized with DensiTree v2.2.6 (Bouckaert, 2010) discarding the first 10% of each MCMC chain as burn-in. A maximum clade credibility tree was then generated using TreeAnnotator (Drummond et al., 2012) and visualized in FigTree v.1.4.3 (http://tree.bio.ed.ac.uk/software/figtree/).

*2.3 mtDNA barcoding*

A mitochondrial phylogeny based on partial mitogenomes, as well as compilation of mtDNA barcoding sequences of the widely used genes 16S and ND3, were recently provided (Dufresnes et al., 2025). To assess how the retrieved genomic patterns relate to mitochondrial diversity, we reported the mitochondrial tree of that recent study and harvested the barcoding sequences they assigned to *D. himalayanus*. These consist of 23 sequences, all from the 16S rRNA gene, of which 11 were geo-referenced (6 localities). To visualize the variation, we constructed a haplotype network with Hapsolutely (Vences et al., 2024) based on an alignment of 443 bp after trimming edge sites with unidentified bases.

*2.4 Species distribution modelling*

To construct species distribution models (SDMs), species occurrence records were compiled from our *D. himalayanus* samples used for molecular analyses (see above) and from georeferenced museum specimens deposited at the MNHN. All records were evaluated for accuracy by mapping them in DIVA-GIS 7.5 (Hijmans et al., 2005). Records from the potential contact zone—specifically those located directly along the Kali Gandaki River—were excluded to avoid potential artifacts from hybridization. A total of 63 occurrence records remained, with the western lineage accounting for 70 % (44 records) and the eastern lineage for 30% (19 records), which were used for niche modeling and potential distribution analyses (Supplementary Material Table S2).

As spatial environmental predictors, we obtained 19 bioclimatic variables representing present-day conditions (1979–2013) from the CHELSA database v2.1 (Karger et al., 2018) at a spatial resolution of 2.5 arc minutes. To minimize collinearity among variables, we retained only one predictor from each pair with a Spearman's rank correlation coefficient exceeding |0.75|. The final selection included variables relevant to temperature and water availability—factors particularly important for amphibians. These comprised: annual mean temperature (bio1), annual precipitation (bio12), precipitation of the driest month (bio14), precipitation seasonality (bio15), precipitation of the warmest quarter (bio18), and precipitation of the coldest quarter (bio19).

We also incorporated paleoclimatic data for two historical periods: the mid-Pliocene Warm Period (mPWP v1.0, ~3.205 Ma) (Hill, 2015), and the mid-Pliocene Cooling Period (Marine Isotope

Stage M2 v1.0, ~3.3 Ma) (Dolan et al., 2015), both downloaded from the Paleoclimate Database (Brown et al., 2018) at the same resolution of 2.5 arc minutes.

SDMs and model fitting were conducted using MaxEnt version 3.4.4 (Phillips et al., 2017a; Phillips and Dudík, 2008; Phillips et al., 2017b). As environmental background, we selected an area defined by a minimum convex polygon enclosing the eastern respective western species records, which was buffered by 50 km and clipped to the WWF ecoregions sensu Olsen et al. (Olson et al., 2001) in which the species records were situated. Model optimization was guided by the corrected Akaike Information Criterion (AICc), following the approach outlined in a previous study (Ginal et al., 2022). We tested various regularization parameters from 0.5 to 5 in steps of 0.1 and all possible combinations of feature classes, which were recommended for the respective number of records (linear, quadratic and hinge). More complex feature classes were omitted as their use may result in over complex models, in which the number of parameters likely exceeds the number of species records. For each combination, 100 models were computed using 80% of the records for model training and the remaining records for model testing. For each model, AUC as well as AICc was computed. We selected the best settings based on AUCtest > 0.7 and the lowest AICc. Using these settings, we computed the final models using the same data split. Model performance was assessed using AUC, the continuous Boyce Index (Boyce et al., 2002; Hirzel et al., 2006) and the true skill statistics (Allouche et al., 2006) in ecospat for R (Broennimann et al., 2025). To assess areas with potentially novel environmental conditions—those outside the range used in model training—we employed Multivariate Environmental Similarity Surface (MESS) analysis (Elith et al., 2010).

*2.5 Niche overlap, similarity and equivalency*

For multivariate climatic niche overlap analysis between the east and west lineage of *D. himalayanus*, we applied the *PCA-env* method (Broennimann et al., 2012), which accounts for the availability of specific environmental conditions within each lineage's accessible area. These accessible areas were defined as buffers with a 50 km radius surrounding each set of occurrence records. Among various available methods, the *PCA-env* approach has been demonstrated to be particularly effective for quantifying niche overlap (Broennimann et al., 2012; Petitpierre et al., 2012).

As a measure of overlap, this method uses Schoener's D (Schoener, 1970), a widely accepted metric for ecological niche comparisons (Rödder and Engler, 2011; Warren et al., 2008), which ranges from 0 (no overlap) to 1 (complete overlap).

Significance of the *PCA-env* results was evaluated using the niche equivalency and niche similarity tests (Broennimann et al., 2012; Warren et al., 2008). Both tests are widely used in ENM and have been described in detail elsewhere (Broennimann et al., 2012; Rödder and Engler, 2011). The niche equivalency test examines whether the environmental niches derived from two species (or lineage) occurrence datasets are statistically indistinguishable (i.e., niches are equal). This is done by comparing the observed niche overlap with a null distribution generated through randomization, using a one-tailed test at a 95% confidence level (CI). In contrast, the niche similarity test evaluates whether the observed overlap is greater than would be expected given the environmental conditions available within one species' accessible area. This test is two-tailed and conducted separately for each species or lineage, with a confidence interval of 0.025–0.975. We did not consider niche dynamic indices (niche stability, unfilling, and expansion) because they were originally introduced in studies on invasive species that are still in the process of expanding their range.

## 3. Results

### *3.1 ddRAD-seq analyses*

Phylogenomic analyses retrieved the focal species *D. himalayanus* (n = 31) and the outgroup *D. melanostictus* (n = 5) as two separate clades, (Fig. 2). In *D. himalayanus*, two deeply diverged, fully supported nuclear lineages are distinguished, one occurring west of the Thakkhola Basin (Kali Gandaki River, West Nepal, Northwest India), and one occurring east of that river valley (Central and East Nepal; continuing further to the East) (Fig. 1, 2).

Clustering analyses of *D. himalayanus* samples (n = 31 from 31 localities) suggested two clusters as the solution that minimizes cross-entropy (Supplementary Material Fig. S1). These clusters correspond to the western and eastern lineages identified by the phylogeny, with the two easternmost samples of the western lineage showing mixed ancestry, consistent with introgression from the eastern lineage (Fig. 2). The PCA confirms the clear-cut separation of the two lineages, which drives PC1,

while PC2 distinguishes the admixed easternmost samples of the western lineage; these are accordingly the most diverged of the western lineage on the phylogenetic tree (Fig. 2). Patterns of observed heterozygosity are relatively homogenous throughout the range, samples from the two lineages sharing similar levels (Fig. 2).

The LEA clustering of *D. himalayanus* and *D. melanostictus* with K = 2 discriminated the two species and assigned all individuals to either group without any signal of mixed ancestry, suggesting a complete absence of interspecific gene flow among our samples (Fig. 3).

Analyses including low-quality Bhutan samples suggest that these belong the eastern lineage (Fig. 4), with some marked genetic differentiation from the other populations of that lineage. On the tree, the two Bhutan samples form a diverged lineage within the eastern lineage (Fig. 4). In the clustering inference, these samples are unambiguously grouped with samples from eastern lineage when two clusters are defined (K = 2, which as above distinguishes the eastern vs western lineages), but they form their own cluster when a third group is allowed (K = 3) (Fig. 4), noting that the latter solution minimizes the cross-entropy (Supplementary Material Fig. S1). The distinction of three groups is also clearly supported by the PCA (Fig. 4).

The species timetree analysis retrieved the Time to Most Recent Common Ancestor (TMRCA) of *D. himalayanus* and *D. melanostictus* close to the calibration prior, namely 9.9 Mya (95% Highest Probability Density (HPD): 6.5–14.0 Mya, Fig. 5). The divergence between the eastern and western lineages of *D. himalayanus* was then estimated to 3.2 Mya (95% HPD: 2.0–4.4 Mya, Fig. 5).

*3.2 mtDNA analyses*

Variation at the 16S rRNA gene [sequences compiled from Dufresnes et al. (2025)] confirms the mitochondrial divergence between western and eastern *D. himalayanus* populations, with the distribution of lineages fully consistent with the nuclear results (Fig. 6).

*3.3 Niche modelling* of the *D. himalayanus* lineages

The PCA identified two main components that together account for 83.5% of the total variance in the environmental dataset (Table 1). Component 1 explains 53.1% of the variance and is primarily influenced by strong positive loadings of annual mean temperature (bio1), annual precipitation (bio12), precipitation seasonality (bio15), and precipitation of the warmest quarter (bio18), while it shows a marked negative association with precipitation of the coldest quarter (bio19). PC1 seems to reflect a general climatic gradient related to overall temperature and precipitation patterns, particularly annual averages and seasonal variability. Component 2 explains an additional 30.4% of the variance and is characterized by strong negative contributions from precipitation of the driest month (bio14), precipitation of the coldest quarter (bio19), annual precipitation (bio12), and precipitation of the warmest quarter (bio18). These loadings suggest that Component 2 likely captures variation related to aridity and dry season conditions. The potential variable distributions are mainly driven by annual mean temperature and annual precipitation (Supplementary Material Table S3 and Fig. S2).

Our niche analysis indicates that the two lineages occupy no or very limited overlapping environmental niche (Fig. 7A), according to the categorization of Rödder and Engler (2011). The niche similarity test yielded a result approaching significance (Schoener's D = 0.17, p = 0.066; Fig. 7B), suggesting a possible tendency toward ecological conservatism between the two lineages; however, the observed overlap does not significantly exceed expectations under a null model of random background similarity. A significant result in this test would imply that observed differences are more likely driven by climate space than by intrinsic ecological divergence. This pattern, however, is inconsistent with the result of the niche equivalency test (p = 0.66), which fails to reject the null hypothesis of equivalent niches. In summary, ENM reveals differences in climatic space (especially precipitation), but not necessarily ecological divergence.

The present-day SDMs performed well and exhibited high predictive accuracy in terms of AUC, TSS and Boyes index statistics (Table 2). Figure 8A-F displays both present SDM projections for the eastern and western lineages, based on ecological niche modeling.

During the cooling period M2 (*ca*. 3.3 Mya), projections indicate disjunct suitable habitat patches west of the upper Kali Gandaki River for the eastern lineage, and very limited areas to the east

of the river and in the eastern Himalaya for both lineages (Fig. 8C, F). In contrast, projections for the warm mid-Pliocene warm period (mPWP) suggest a substantial shift in suitable habitats toward the eastern and northeastern margins of the present-day Tibetan Plateau, with a broader extent for the western lineage compared to the eastern one (Fig. 8B, E). Notably, during mPWP, the projected ranges for both lineages in the Himalaya are limited to a few isolated areas—east and west of the Kali Gandaki River, as well as between the Arun and Tama Koshi rivers in eastern Nepal (western lineage), and in the eastern Himalaya of Arunachal Pradesh (both lineages).

The present-day projections (Fig. 8A, D) closely align with the known geographic distribution of *D. himalayanus* but also predict extensive suitable habitats beyond the documented range, particularly in the eastern Himalaya and farther south into Indochina.

## 4. Discussion

This study combines genomic phylogeography with ecological niche analyses for *D. himalayanus* to reconstruct its biogeographic history across the Himalaya.

### *4.1 Diversification of* Duttaphrynus himalayanus

Phylogenomic analyses confirm the monophyly of *D. himalayanus* relative to *D. melanostictus*, with a Late Miocene divergence (Dufresnes et al., 2025). This time frame coincides with major phases of Himalayan orogeny (Fort, 1996; Spicer et al., 2024; Wang et al., 1982; Wang et al., 2025), suggesting that uplift-related environmental changes likely promoted the split between highland (*D. himalayanus*) and lowland (*D. melanostictus*) lineages. The divergence thus may mark both the minimum age for the emergence of suitable montane habitats (providing conditions necessary for the evolution of *D. himalayanus*) and the timescale needed for Himalayan amphibians to adapt to high-elevation conditions, which typically occurs over millions of years (Hutter et al., 2017; Navas, 2006; Sun et al., 2015).

Within *D. himalayanus*, we identified at least two Pliocene lineages (~3.2 Mya), separated geographically by the Thakkhola Basin, the upstream area of the Kali Gandaki River. Ecological niche modeling indicated differentiation in climatic space, particularly in precipitation-related variables,

while showing extensive elevational overlap. This pattern points to allopatric divergence driven by topographic barriers rather than ecological differentiation, indicating niche conservatism in temperature-related factors. Given their occupancy of similar elevational zones, these two lineages may be experiencing an early stage of speciation initiated by the extreme relief dynamics of the Kali Gandaki River valley. This valley, the deepest in the world (6,000–7,000 m), separates Dhaulagiri (8,167 m a.s.l.) to the west from Annapurna (8,091 m a.s.l.) to the east. The pronounced climatic gradients along its elevational zones, including a distinct dry-valley stage (Miehe, 2015) likely represent the actual climatic, and, thus, dispersal barrier, with limited or no contact to date. Despite this, evidence of introgression across the phylogeographic break suggests that this barrier is leaky across time, allowing occasional gene flow. Such permeability may reflect temporary paleogeographic changes, such as the formation of paleolakes following large-scale landslides during the Late Pleistocene and Holocene (Fort, 2000). These ephemeral lakes may have created transient dispersal corridors, enabling secondary contact between eastern and western lineages that are otherwise isolated by the gorge. Whether these lineages represent incipient species remains uncertain, but their structure illustrates how Himalayan topography and paleogeographic instability can repeatedly generate and partially reconnect evolutionary lineages. Testing for speciation could involve assessing these barriers, by examining patterns of gene flow in the identified phylogeographic transition, and/or assessing lineage-specific phenotypic adaptations.

Within the eastern lineage, additional genetic structuring may point to a younger divergence that is potentially associated with the Arun River valley in East Nepal, another major north–south incision of the Himalaya. This river system might have functioned as a secondary isolating barrier, particularly during interglacial periods when *D. himalayanus* may have recolonized higher elevations following possible downhill range contractions during glacial maxima. Such repeated elevational shifts could potentially have fostered cycles of isolation and contact, gradually driving population divergence (Fig. 4) while maintaining a degree of genetic connectivity across the range.

Ecological niche models further indicate that *D. himalayanus* remains tightly associated with montane forests, which likely restricted post-divergence expansion into lowlands and reinforced isolation from *D. melanostictus*. A recurring hypothesis in the literature posits the existence of a

hybrid zone where the vertical distribution ranges of the two species overlap along the Himalayan arc (Nanhoe and Ouboter, 1987; Schleich and Kästle, 2002). However, the absence of introgression between sympatric populations of these two species contradicts this idea and instead supports long-term reproductive isolation, probably maintained by a combination of climatic specialization, topographic barriers, and reproductive incompatibilities.

### *4.2 Taxonomic implications*

Our findings imply that taxonomic revisions in *D. himalayanus* are required, as the observed genomic structure indicates the presence of at least two evolutionary lineages within what is currently regarded as a single species. In the original description of this taxon, Günther (1864) mentioned several specimens from "Sikkim and Nepal" without further precision. Later, Boulenger (1882) listed seven specimens from Nepal, Sikkim, and Darjeeling—without explicitly designating any as types—and illustrated one of them, BMNH 1858.6.24.1, an adult male collected by B. Hodgson in Nepal. Subsequently, Dubois and Ohler (1999) designated this specimen as the lectotype, thereby fixing the type locality as Nepal. Based on the lectotype's origin and the fact that most of Hodgson's collections were made in and around the Kathmandu Valley, Dubois and Ohler (1999) concluded that the specimen most probably originated from Mount Phulchoki, southeast of Kathmandu. Accordingly, the type locality of *D. himalayanus* is probably situated east of the Kali Gandaki River and may therefore correspond to the eastern genetic lineage identified in this study.

### *4.3 Origin of* Duttaphrynus himalayanus *in the Himalaya*

The origin of *D. himalayanus* can be viewed within three main biogeographic hypotheses: (i) east-to-west colonization from Indochina (Martens, 2015), (ii) a paleo-Tibetan origin (Schmidt et al., 2012) with subsequent southward range shifts driven by uplift-related climate change, as suggested for high-montane Himalayan amphibians like *Nanorana* Günther, 1896 and *Scutiger* Theobald, 1868 (Hofmann et al., 2024a; Hofmann et al., 2024b), or (iii) in situ diversification from sub-Himalayan ancestors following orogenic uplift.

The species' closest relatives include *D. melanostictus* and other taxa from the Indian subcontinent (Dufresnes et al., 2025), with *D. himalayanus* forming a sister relationship specifically with *D. beddomii* (Günther, 1876), a species endemic to the Western Ghats of India (Wu et al. 2025). Phylogenomic analyses of *D. melanostictus* further revealed that true *D. melanostictus* is restricted to the Indian subcontinent and is closely allied to Western Ghats species, whereas populations from Southeast Asia represent a distinct, cryptic lineage (Dufresnes et al., 2025). Interestingly, mitochondrial data from *D. melanostictus* populations in Pakistan, Nepal, and northern India show deeply divergent lineages with affinities to Southeast Asian taxa., possibly reflecting an extinct Himalayan form of eastern origin. These findings may support a long and complex biogeographic history for the *D. melanostictus/himalayanus* clade in the Himalayan region, which is consistent with the hypothesis that *D. himalayanus* derived from a montane-adapted ancestor at the southern margin of the Himalaya-Tibet orogen. As a result of the geomorphological evolution of the Greater Himalaya, subtropical to temperate habitats became widespread along the Himalayan foothills and transverse valleys, allowing these ancestral populations to expand their range. The uplift of the Himalayas therefore led to a gradual southward shift of the original distribution area. Potential local range contractions during glacial cooling phases to lower elevations, followed by repeated range expansions—most likely along transverse valleys—toward higher elevations during interglacial warm periods, can also be assumed. Under this scenario, ancestral populations tracked rising terrain and suitable climates upslope, diversifying along the Himalayan arc as the range uplifted. Their relatively shallow phylogenetic divergence, except across the Kali Gandaki break, supports a recent and dynamic diversification rather than an ancient Miocene radiation. The species' notable dispersal capability likely facilitated range continuity across most north–south valleys, except the deepest gorges.

This pattern contrasts with a paleo-Tibetan origin, which would predict multiple Miocene lineages structured by major topographic features such as the Himalayan subranges or its large transverse river valleys, as observed in genera such as *Nanorana* and *Scutiger* (Hofmann et al., 2019; Hofmann et al., 2024a; Hofmann et al., 2017). However, apart from the split between its eastern and western lineages, and in some lower, in the Bhutan populations, *D. himalayanus* exhibits relatively

shallow phylogenetic divergence—suggesting a more recent diversification pattern inconsistent with the deep temporal and spatial structuring expected under a paleo-Tibetan origin scenario.

An east-to-west dispersal from Indochina during the Late Miocene also appears unlikely, since the species is absent from the eastern margin of the Tibetan Plateau, where suitable habitats exist and likely persisted through the Pliocene (~ 3 Mya; Fig. 8A-D). Reconciling this with an east-to-west migration would require invoking a widespread, undocumented extinction of eastern populations without genetic traces or subsequent recolonization—an implausible set of assumptions. The region should have provided stable habitats for montane amphibians throughout Pliocene climatic fluctuations (Zhang et al., 2010; Zheng et al., 2020), as supported by our SDMs, which indicate that suitable environments persisted not only within the Himalaya but also along the eastern plateau margins (Fig. 8C and F).

Therefore, the most parsimonious explanation is that *D. himalayanus* originated within the rising Himalaya from a sub-Himalayan ancestor, with diversification driven by the interplay of uplift dynamics, topographic barriers, and Pleistocene climatic oscillations.

## 5. Conclusions

Our phylogeographic and ecological analyses reveal that *Duttaphrynus himalayanus* represents a young montane lineage–compared to other Himalayan amphibians (Hofmann et al. 2019, 2024a, b; Xu et al. 2020)–that diversified within the rising Himalaya. The species comprises two Pliocene lineages separated by the Kali Gandaki Valley in west-central Nepal, and a younger divergence within the eastern lineage likely associated with the Arun River valley in eastern Nepal or Quaternary range contractions and subsequent upslope recolonization. Climatic niche modeling indicates that divergence was primarily driven by topographic barriers rather than by ecological differentiation.

The most plausible origin scenario places *D. himalayanus* as a derived lineage from sub-Himalayan ancestors that expanded upslope in response to orogenic uplift, rather than as a relict of a paleo-Tibetan or Indochinese lineage. Overall, the evolutionary history of *D. himalayanus* exemplifies

how the interaction of uplift, topography, and climatic change has shaped the diversification of Himalayan montane biotas.

**CRediT authorship contribution statement**

S.H. and C.D. contributed jointly to the study design, interpretation and original draft. C.D., D.R., and SH analyzed the data; J.S., M.F., D.J., A.D., A.O., C.B.B., V.V., and S.L. contributed to the investigation and provided resources. All authors read and approved the final manuscript.

**Declaration of competing interest**

The authors declare that they have no known competing financial interests or personal relationships that could have appeared to influence the work reported in this paper.

**Acknowledgements**

The authors acknowledge M. Vences (Technische Universität Braunschweig, Braunschweig, Germany) for molecular lab facilities and lab support, M. Hartmann and K. Kürbis (NHME) for accessioning specimens, and Svetlana Vershinina (†2021) for assistance in the field.

**Funding**

This work was supported by the Deutsche Forschungsgemeinschaft (DFG grant HO3792/8-1 to SH) and by the Institute of Plant and Animal Ecology, Ural Branch of the Russian Academy of Sciences within the state assignment of the Ministry of Science and Higher Education, Russian Federation (grant No. 122021000082-0 to VV). The funding body played no role in the design of the study and collection, analysis, interpretation of data, and in writing the manuscript.

**Appendix A. Supplementary data**

Supplementary data to this article:

Table S1. Details on the samples used in this study.

Table S2. Occurrence records (WGS84) of the eastern (E) and western (W) lineages of *D. himalayanus* used in species distribution modeling.

Table S3. Percent contribution of bioclimatic variables to MaxEnt models for *D. himalayanus* in eastern (E) and western (W) regions.

Figure S1. Cross-entropy estimates from the LEA analyses on the main dataset (left) and the subdata designed to assess the Bhutan samples (right).

Figure S2. Response curves for the eastern (E) and western (W) lineages of *D. himalayanus* generated from MaxEnt models. The curves show the relationship between habitat suitability (logistic output) and key bioclimatic variables (bio1 = annual mean temperature, bio12 = annual precipitation, bio14 = precipitation of driest month, bio15 = precipitation seasonality, bio18 = precipitation of warmest quarter, bio19 = precipitation of coldest quarter). The red line represents the mean response, and the blue shading indicates ±1 standard deviation across model replicates.

**Data availability** – Raw ddRAD sequencing reads have been archived on NCBI SRA under BioProject RJNA949685 and mtDNA sequences have been deposited on GenBank; accessions, voucher and locality data are listed in Supplementary Material Table S1. Species records for SDM are provided in Supplementary Material Table S2.

**References**

Ahrens, D., 2004. Phylogeny and zoogeography of the Sericini in the Himalayan region (Insecta: Coleoptera: Scarabaeidae). University of Berlin, Berlin, p. 193.

Allouche, O., Tsoar, A., Kadmon, R., 2006. Assessing the accuracy of species distribution models: prevalence, kappa and the true skill statistic (TSS). J. Appl. Ecol. 43, 1223–1232. https://doi.org/10.1111/j.1365-2664.2006.01214.x

Bouckaert, R.R., 2010. DensiTree: making sense of sets of phylogenetic trees. Bioinformatics 26, 1372–1373. https://doi.org/10.1093/bioinformatics/btq110

Boulenger, G.A., 1882. Catalogue of the Batrachia Salientia s. Ecaudata in the Collection of the British Museum Second Edition ed. Taylor and Francis, London.

528 Boyce, M.S., Vernier, P.R., Nielsen, S.E., Schmiegelow, F.K.A., 2002. Evaluating resource selection
529 functions. Ecol. Model. 157, 281–300. https://doi.org/10.1016/S0304-3800(02)00200-4
530 Broennimann, O., Di Cola, V., Guisan, A., 2025. ecospat: Spatial Ecology Miscellaneous Methods. R
531 package version 4.1.2, https://github.com/ecospat/ecospat.
532 Broennimann, O., Fitzpatrick, M.C., Pearman, P.B., Petitpierre, B., Pellissier, L., Yoccoz, N.G.,
533 Thuiller, W., Fortin, M.-J., Randin, C., Zimmermann, N.E., Graham, C.H., Guisan, A., 2012.
534 Measuring ecological niche overlap from occurrence and spatial environmental data. Glob. Ecol.
535 Biogeogr. 21, 481–497. https://doi.org/10.1111/j.1466-8238.2011.00698.x
536 Bryant, D., Bouckaert, R., Felsenstein, J., Rosenberg, N.A., RoyChoudhury, A., 2012. Inferring
537 species trees directly from biallelic genetic markers: bypassing gene trees in a full coalescent
538 analysis. Mol. Biol. Evol. 29, 1917–1932. https://doi.org/10.1093/molbev/mss086
539 Catchen, J., Hohenlohe, P.A., Bassham, S., Amores, A., Cresko, W.A., 2013. Stacks: an analysis tool
540 set for population genomics. Mol. Ecol. 22, 3124–3140. https://doi.org/10.1111/mec.12354
541 Cerca, J., Maurstad, M.F., Rochette, N.C., Rivera-Colón, A.G., Rayamajhi, N., Catchen, J.M., Struck,
542 T.H., 2021. Removing the bad apples: A simple bioinformatic method to improve loci-recovery
543 in de novo RADseq data for non-model organisms. Methods Ecol. Evol. 12, 805–817.
544 https://doi.org/10.1111/2041-210X.13562
545 Cun, Y.Z., Wang, X.Q., 2010. Plant recolonization in the Himalaya from the southeastern Qinghai-
546 Tibetan Plateau: Geographical isolation contributed to high population differentiation. Mol.
547 Phylogenet. Evol. 56, 972–982. https://doi.org/10.1016/j.ympev.2010.05.007
548 Dolan, A.M., Haywood, A.M., Hunter, S.J., Tindall, J.C., Dowsett, H.J., Hill, D.J., Pickering, S.J.,
549 2015. Modelling the enigmatic Late Pliocene Glacial Event — Marine Isotope Stage M2. Glob.
550 Planet. Change 128, 47–60. https://doi.org/10.1016/j.gloplacha.2015.02.001
551 Drummond, A.J., Suchard, M.A., Xie, D., Rambaut, A., 2012. Bayesian phylogenetics with BEAUti
552 and the BEAST 1.7. Mol. Biol. Evol. 29, 1969–1973. https://doi.org/10.1093/molbev/mss075
553 Dubois, A., Ohler, A., 1999. Asian and Oriental toads of the *Bufo melanostictus, Bufo scaber* and *Bufo*
554 *stejnegeri* groups (Amphibia, Anura): a list of available and valid names and redescription of
555 some name-bearing types. J. South Asian Nat. Hist. Colombo 4, 133–180.

Dufresnes, C., Jablonski, D., Ambu, J., Prasad, V.K., Bala Gautam, K., Kamei, R.G., Mahony, S., Hofmann, S., Masroor, R., Alard, B., Crottini, A., Edmonds, D., Ohler, A., Jiang, J., Khatiwada, J.R., Gupta, S.K., Borzee, A., Borkin, L.J., Skorinov, D.V., Melnikov, D.A., Milto, K.D., Konstantinov, E.L., Kunzel, S., Suchan, T., Arkhipov, D.V., Trofimets, A.V., Nguyen, T.V., Suwannapoom, C., Litvinchuk, S.N., Poyarkov, N.A., 2025. Speciation and historical invasions of the Asian black-spined toad (*Duttaphrynus melanostictus*). Nat. Commun. 16, 298. https://doi.org/10.1038/s41467-024-54933-4

Elith, J., Kearney, M., Phillips, S.J., 2010. The art of modelling range-shifting species. Methods in Ecology and Evolution 1, 330–342. http://www.respond2articles.com/MEE/

Fei, L., Ye, C.J., Jiang, J.P., 2012. Colored Atlas of Chinese Amphibians and Their Distributions. Sichuan Science and Technology Press, Sichuan, China.

Fort, M., 1996. Late Cenozoic environmental changes and uplift on the northern side of the central Himalaya: a reappraisal from field data. Palaeo3 120, 123–145. https://doi.org/10.1016/0031-0182(94)00038-7

Fort, M., 2000. Glaciers and mass wasting processes: their influence on the shaping of the Kali Gandaki valley (higher Himalaya of Nepal). Quatern. Int. 65/66, 101–119. https://doi.org/10.1016/S1040-6182(99)00039-7

Frichot, E., François, O., 2015. LEA: An R package for landscape and ecological association studies. Methods Ecol. Evol. 6, 925–929. https://doi.org/10.1111/2041-210X.12382

Ginal, P., Tan, W.C., Rödder, D., 2022. Invasive risk assessment and expansion of the realized niche of the *Calotes versicolor* species complex (Daudin, 1802). Front. Biogeogr. 14.3, e54299.

Günther, A.C.L.G., 1864. The Reptiles of British India. London: Ray Society by R. Hardwicke. Ray Society by R. Hardwicke, London.

Hijmans, R.J., Guarino, L., Jarvis, A.O., Brien, R., Mathur, P., Cruz, C.B.M., Barrantes, I., Rojas, E., 2005. DIVA-GIS Version 5.2 Manual. 1–73.

Hill, D.J., 2015. The non-analogue nature of Pliocene temperature gradients. Earth and Planetary Sci. Lett. 425, 232–241. https://doi.org/10.1016/j.epsl.2015.05.044

583 Hirzel, A.H., Le Lay, G., Helfer, V., Randin, C., Guisan, A., 2006. Evaluating the ability of habitat
584 suitability models to predict species presences. Ecol. Model. 199, 142–152.
585 https://doi.org/10.1016/j.ecolmodel.2006.05.017
586 Hofmann, S., Baniya, C.B., Litvinchuk, S.N., Miehe, G., Li, J.T., Schmidt, J., 2019. Phylogeny of
587 spiny frogs *Nanorana* (Anura: Dicroglossidae) supports a Tibetan origin of a Himalayan species
588 group. Ecol. Evol. 9, 14498–14511. https://doi.org/10.1002/ece3.5909
589 Hofmann, S., Podsiadlowski, L., Andermann, T., Matschiner, M., Baniya, C.B., Litvinchuk, S.N.,
590 Martin, S., Masroor, R., Yang, J., Zheng, Y., Jablonski, D., Schmidt, J., 2024a. The last of their
591 kind: Is the genus *Scutiger* (Anura: Megophryidae) a relict element of the paleo-Transhimalaya
592 biota? Mol. Phylogenet. Evol. 201, 108166. https://doi.org/10.1016/j.ympev.2024.108166
593 Hofmann, S., Rodder, D., Andermann, T., Matschiner, M., Riedel, J., Baniya, C.B., Flecks, M., Yang,
594 J., Jiang, K., Jianping, J., Litvinchuk, S.N., Martin, S., Masroor, R., Nothnagel, M., Vershinin,
595 V., Zheng, Y., Jablonski, D., Schmidt, J., Podsiadlowski, L., 2024b. Exploring Paleogene Tibet's
596 warm temperate environments through target enrichment and phylogenetic niche modelling of
597 Himalayan spiny frogs (Paini, Dicroglossidae). Mol. Ecol. 33, e17446.
598 https://doi.org/10.1111/mec.17446
599 Hofmann, S., Stoeck, M., Zheng, Y., Ficetola, F.G., Li, J.T., Scheidt, U., Schmidt, J., 2017. Molecular
600 Phylogenies indicate a Paleo-Tibetan Origin of Himalayan Lazy Toads (*Scutiger*). Sci. Rep. 7,
601 3308. https://doi.org/10.1038/s41598-017-03395-4
602 Hutter, C.R., Lambert, S.M., Wiens, J.J., 2017. Rapid Diversification and Time Explain Amphibian
603 Richness at Different Scales in the Tropical Andes, Earth's Most Biodiverse Hotspot. Am. Nat.
604 190, 828–843. https://doi.org/10.1086/694319
605 Johansson, U.S., Alstrom, P., Olsson, U., Ericson, P.G.R., Sundberg, P., Price, T.D., 2007. Build-up of
606 the Himalayan avifauna through immigration: A biogeographical analysis of the *Phylloscopus*
607 and *Seicercus* warblers. Evol. 61, 324–333. https://doi.org/10.1111/j.1558-5646.2007.00024.x
608 Jombart, T., 2008. adegenet: a R package for the multivariate analysis of genetic markers. Bioinform.
609 24, 1403–1405. https://doi.org/10.1093/bioinformatics/btn129

Kapp, P., DeCelles, P.G., Leier, A.L., Fabijanic, J.M., He, S., Pullen, A., Gehrels, G.E., 2007. The Gangdese retroarc thrust belt revealed. GSA Today 17, 4–9.

Karger, D.N., Conrad, O., Böhner, J., Kawohl, T., Kreft, H., Soria-Auza, R.W., Zimmermann, N.E., Linder, H.P., Kessler, M., 2018. Climatologies at high resolution for the earth's land surface areas. Sci. Data 4, 170122. https://doi.org/10.1038/sdata.2017.122

Kathiwada, J.R., Wang, B., Zhao, T., Xie, F., Jiang, J., 2021. An integrative taxonomy of amphibians of Nepal: An updated status and distribution. Asian Herpetol. Res. 12, 1–35. https://doi.org/10.16373/j.cnki.ahr.200050

Litvinchuk, S.N., 2011. Molecular-genetic analysis of evolution of North-Palearctic amphibians, in: Issues of Herpetology: Materials of the Fourth Congress of the A.M. Nikolsky Herpetological Society. Saint Petersburg. P. 154–161. [In Russian].

Liu, H.R., Gao, Q.B., Zhang, F.Q., Khan, G., Chen, S.L., 2018. Westwards and northwards dispersal of *Triosteum himalayanum* (Caprifoliaceae) from the Hengduan Mountains region based on chloroplast DNA phylogeography. PeerJ 6, e4748. https://doi.org/10.7717/peerj.4748

Mani, M.S., 1986. Butterflies of the Himalaya. Springer Dordrecht, Dordrecht, The Netherlands.

Martens, J., 1993. Bodenlebende Arthropoden im zentralen Himalaya: Bestandsaufnahme, Wege zur Vielfalt und ökologische Nischen, in: Schweinfurth, U. (Ed.), Neue Forschungen im Himalaya. Steiner, Stuttgart, pp. 231–250.

Martens, J., 2015. Fauna – Himalayan patterns of diversity, in: Miehe, S., Pendry, C. (Eds.), Nepal. An introduction to the natural history, ecology and human environment in the Himalayas. A companion to the Flora of Nepal. Royal Botanic Garden Edinburgh, Edinburgh, pp. 168–173.

Miehe, G., 2015. 15. Ecological Transects: 15.2 Kali Gandaki, in: Miehe, G., Pendry, C. (Eds.), Nepal - An Introduction to the Natural History, Ecology and Human Impact of the Himalayas. Royal Botanic Garden Edinburgh, Edinburgh, pp. 347–357.

Minh, B.Q., Schmidt, H.A., Chernomor, O., Schrempf, D., Woodhams, M.D., von Haeseler, A., Lanfear, R., 2020. IQ-TREE 2: New Models and Efficient Methods for Phylogenetic Inference in the Genomic Era. Mol. Biol. Evol. 37, 1530–1534. https://doi.org/10.1093/molbev/msaa015

637 Mittermeier, R.A., Robles Gil, P., Hoffman, M., Pilgrim, J., Brooks, T., Mittermeier, C.G., Lamoreux,
638 J., da Fonseca, G.A.B., 2004. Hotspots Revisited. CEMEX, Mexico City.
639 Mittermeier, R.A., Turner, W.R., Larsen, F.W., Brooks, T.M., Gascon, C., 2011. Global Biodiversity
640 Conservation: The Critical Role of Hotspots, in: Zachos, F.E., Habel, J.C. (Eds.), Biodiversity
641 Hotspots. Springer, Berlin Heidelberg pp. 3–22.
642 Murphy, M.A., Yin, A., Harrison, T.M., Durr, S.B., Chen, Z., Ryerson, F.J., Kidd, W.S.F., Wang, X.,
643 Zhou, X., 1997. Did the Indo-Asian collision alone create the Tibetan plateau? Geology 25, 719–
644 722. https://doi.org/10.1130/0091-7613(1997)025%3C0719:DTIACA%3E2.3.CO;2
645 Nanhoe, L.M.R., Ouboter, P.E., 1987. The distribution of reptiles and amphibians in the Annapurna-
646 Dhaulagiri region (Nepal). Zool. Verh. 240, 1–100.
647 Navas, C.A., 2006. Patterns of distribution of anurans in high Andean tropical elevations: Insights
648 from integrating biogeography and evolutionary physiology. Integr. Comp. Biol. 46, 82–91.
649 https://doi.org/10.1093/icb/icj001
650 Olson, D.M., Dinerstein, E., Wikramanayake, E.D., Burgess, N.D., Powell, G.V., Underwood, E.C.,
651 D'amico, J.A., Itoua, I., Strand, H.E., Morrison, J.C., Loucks, C.J., Allnutt, A.F., Ricketts, T.H.,
652 Kura, Y., Lamoreux, J.F., Wettengel, W.W., Hedao, P., Kassem, K.R., 2001. Terrestrial
653 ecoregions of the world: a new map of life on earth - A new global map of terrestrial ecoregions
654 provides an innovative tool for conserving biodiversity. Biosci. 51, 933–938.
655 https://doi.org/10.1641/0006-3568(2001)051[0933:TEOTWA]2.0.CO;2
656 Othman, S.N., Chen, Y.H., Chuang, M.F., Andersen, D., Jang, Y., Borzee, A., 2020. Impact of the
657 Mid-Pleistocene Revolution and Anthropogenic Factors on the Dispersion of Asian Black-Spined
658 Toads (Duttaphrynus melanostictus). Animals (Basel) 10.
659 Pan, X.-F., Min, R., Nie, X., 2024. Revising palaeoelevation estimates for the Tibetan Plateau by
660 integrating latitude, paleogeographic and paleotemperature data. Palaeo3 647, 112219.
661 https://doi.org/10.1016/j.palaeo.2024.112219
662 Petitpierre, B., C., K., Broennimann, O., Randin, C., Daehler, C., Guisan, A., 2012. Climatic niche
663 shifts are rare among terrestrial plant invaders. Sci. 335, 1344–1348.
664 https://doi.org/10.1126/science.1215933

Phillips, S.J., Anderson, R.P., Dudik, M., Schapire, R.E., Blair, M.E., 2017a. Opening the black box: an open-source release of Maxent. Ecography 40, 887–893. https://doi.org/10.1111/ecog.03049

Phillips, S.J., Dudík, M., 2008. Modeling of species distributions with Maxent: New extensions and comprehensive evaluation. Ecography 31, 161–175. https://doi.org/10.1111/j.0906-7590.2008.5203.x

Phillips, S.J., Dudík, M., Schapire, R.E., 2017b. Maxent software for modeling species niches and distributions (Version 3.4.1). Available from url: http://biodiversityinformatics.amnh.org/open_source/maxent/

Rödder, D., Engler, J.O., 2011. Quantitative metrics of overlaps in Grinnellian niches: advances and possible drawbacks. Glob. Ecol. Biogeogr. 20, 915–927. https://doi.org/10.1111/j.1466-8238.2011.00659.x

Rowley, D.B., Currie, B.S., 2006. Palaeo-altimetry of the late Eocene to Miocene Lunpola basin, central Tibet. Nature 439, 677–681. https://doi.org/10.1038/nature04506

Schleich, H.H., Kästle, W., 2002. Amphibians and Reptiles of Nepal. A.R.G. Gantner Verlag, Ruggell.

Schmidt, J., Opgenoorth, L., Holl, S., Bastrop, R., 2012. Into the Himalayan exile: the phylogeography of the ground beetle *Ethira* clade supports the Tibetan origin of forest-dwelling Himalayan species groups. PLoS One 7, e45482. https://doi.org/10.1371/journal.pone.0045482

Schoener, T.W., 1970. Nonsynchronous spatial overlap of lizards in patchy habitats. Ecology 51, 408–418. https://doi.org/10.2307/1935376

Spicer, R.A., Farnsworth, A., Su, T., Ding, L., Witkowski, C.R., Li, S.-F., Xiong, Z., Zhou, Z., Li, S., Hughes, A.C., Valdes, P.J., Widdowson, M., Zhang, X., He, S., Liu, J., Huang, J., Herman, A.B., Xu, Q., Liu, X., Jin, J., Pancost, R., Lunt, D.J., Zhang, S., 2024. The progressive co-evolutionary development of the Pan-Tibetan Highlands, the Asian monsoon system and Asian biodiversity. Geological Society, London, Special Publications 549, 55–112. https://doi.org/10.1144/SP549-2023-180

Spicer, R.A., Su, T., Valdes, P.J., Farnsworth, A., Wu, F.-X., Shi, G., Spicer, T.E.V., Zhou, Z., 2021a. The topographic evolution of the Tibetan Region as revealed by palaeontology. Paleobiodivers. Paleoenviron. 101, 213–243. https://doi.org/10.1007/s12549-020-00452-1

693 Spicer, R.A., Su, T., Valdes, P.J., Farnsworth, A., Wu, F.-X., Shi, G., V., S.T.E., Zhou, Z., 2021b.
694 Why 'the uplift of the Tibetan Plateau' is a myth? Natl. Sci. Rev. 8, 1–19.
695 https://doi.org/10.1093/nsr/nwaa091
696 Stange, M., Sanchez-Villagra, M.R., Salzburger, W., Matschiner, M., 2018. Bayesian Divergence-
697 Time Estimation with Genome-Wide Single-Nucleotide Polymorphism Data of Sea Catfishes
698 (Ariidae) Supports Miocene Closure of the Panamanian Isthmus. Syst. Biol. 67, 681–699.
699 https://doi.org/10.1093/sysbio/syy006
700 Sun, Y.B., Xiong, Z.J., Xiang, X.Y., Liu, S.P., Zhou, W.W., Tu, X.L., Zhong, L., Wang, L., Wu, D.D.,
701 Zhang, B.L., Zhu, C.L., Yang, M.M., Chen, H.M., Li, F., Zhou, L., Feng, S.H., Huang, C.,
702 Zhang, G.J., Irwin, D., Hillis, D.M., Murphy, R.W., Yang, H.M., Che, J., Wang, J., Zhang, Y.P.,
703 2015. Whole-genome sequence of the Tibetan frog *Nanorana parkeri* and the comparative
704 evolution of tetrapod genomes. Proc. Natl. Acad. Sci. USA 112, E1257–1262.
705 https://doi.org/10.1073/pnas.1501764112
706 Tapponnier, P., Xu, Z.Q., Roger, F., Meyer, B., Arnaud, N., Wittlinger, G., Yang, J.S., 2001. Oblique
707 stepwise rise and growth of the Tibet plateau. Sci. 294, 1671–1677.
708 https://doi.org/10.1126/science.105978
709 Van Bocxlaer, I., Biju, S.D., Loader, S.P., Bossuyt, F., 2009. Toad radiation reveals into-India
710 dispersal as a source of endemism in the Western Ghats-Sri Lanka biodiversity hotspot. BMC
711 Evol. Biol. 9, 131. https://doi.org/10.1186/1471-2148-9-131
712 Vences, M., Patmanidis, S., Schmidt, J.C., Matschiner, M., Miralles, A., Renner, S.S., 2024.
713 Hapsolutely: a user-friendly tool integrating haplotype phasing, network construction, and
714 haploweb calculation. Bioinform. Adv. 4, vbae083. https://doi.org/10.1093/bioadv/vbae083
715 Wambulwa, M.C., Milne, R., Wu, Z.Y., Spicer, R.A., Provan, J., Luo, Y.H., Zhu, G.F., Wang, W.T.,
716 Wang, H., Gao, L.M., Li, D.Z., Liu, J., 2021. Spatiotemporal maintenance of flora in the
717 Himalaya biodiversity hotspot: Current knowledge and future perspectives. Ecol. Evol. 11,
718 10794–10812. https://doi.org/10.1002/ece3.7906
719 Wang, C.-Y., Shi, Y.-L., Zhou, W.-H., 1982. Dynamic uplift of the Himalaya. Nature 298, 553–556.

Wang, C.S., Dai, J., Zhao, X., Li, Y., Graham, S.A., He, D.C., Ran, B., Meng, J., 2014. Outward-growth of the Tibetan Plateau during the Cenozoic: a review. Tectonics 621, 1–43. https://doi.org/10.1016/j.tecto.2014.01.036

Wang, Y., Wang, Y., Schoenbohm, L.M., Wang, W., Fox, M., Zhang, P., 2025. Accelerated Pleistocene exhumation and isostatic uplift along the Himalaya. Glob. Planet. Change 252, 104861. https://doi.org/10.1016/j.gloplacha.2025.104861

Warren, D.L., Glor, R.E., Turelli, M., 2008. Environmental niche equivalency versus conservatism: quantitative approaches to niche evolution. Evolution 62, 2868–2883. https://doi.org/10.1111/j.1558-5646.2008.00482.x

White, A.E., 2016. Geographical Barriers and Dispersal Propensity Interact to Limit Range Expansions of Himalayan Birds. Am. Nat. 188, 99–112. https://doi.org/10.1086/686890

Wogan, G.O., Stuart, B.L., Iskandar, D.T., McGuire, J.A., 2016. Deep genetic structure and ecological divergence in a widespread human commensal toad. Biol. Lett. 12, 20150807. https://doi.org/10.1098/rsbl.2015.0807

Wu, D., Prendini, E., Raxworthy, C.J., Wang, Z., Zhou, W., Chen, J., Suwannapoom, C., Sucharitakul, P., Pie, M.R., Xu, W., Yuan, Z. 2025. Earth history and trait innovation drive the global radiation of modern toads. Proceedings of the Royal Society B: Biological Sciences 292, 20251928. https://doi.org/10.1098/rspb.2025.1928

Xing, Y., Ree, R.H., 2017. Uplift-driven diversification in the Hengduan Mountains, a temperate biodiversity hotspot. Proc. Natl. Acad. Sci. USA 114, E3444–E3451. https://doi.org/10.1073/pnas.1616063114

Xu, Q., Ding, L., Zhang, L., Cai, F., Lai, Q., Yang, D.T., Liu-Zheng, J., 2013. Paleogene high elevations in the Qiangtang Terrane, central Tibetan Plateau. Earth and Planetary Sci. Lett. 362, 31–42. https://doi.org/10.1016/j.epsl.2012.11.058

Xu, W., Dong, W.-J., Fu, T.-T., Gao, W., Lu, C.-Q., Yan, F., Wu, Y.-H., Jiang, K., Jin, J.-Q., Chen, H.-M., Zhang, Y.-P., Hillis, D. M., Che, J. 2020. Herpetological phylogeographic analyses support a Miocene focal point of Himalayan uplift and biological diversification. Natl. Sci. Rev. 8, nwaa263. https://doi.org/10.1093/nsr/nwaa263

748 Zhang, M., Rao, D., Yang, J., Yu, G., Wilkinson, J.A., 2010. Molecular phylogeography and
749 population structure of a mid-elevation montane frog *Leptobrachium ailaonicum* in a fragmented
750 habitat of southwest China. Mol. Phylogenet. Evol. 54, 47–58.
751 https://doi.org/10.1016/j.ympev.2009.10.019
752 Zheng, Y., Dai, Q., Guo, X., Zeng, X., 2020. Dynamics behind disjunct distribution, hotspot-edge
753 refugia, and discordant RADseq/mtDNA variability: insights from the Emei mustache toad. BMC
754 Evol. Biol. 20, 111. https://doi.org/10.1186/s12862-020-01675-8
755
756

## Tables and Legends

**Table 1: Climatic PCA loadings.** Loadings of the bioclimatic variables on the first two principal components (PCs) from the PCA of the *Duttaphrynus himalayanus* climatic dataset. BIO1 = Annual Mean Temperature; BIO12 = Annual Precipitation; BIO14 = Precipitation of Driest Month; BIO15 = Precipitation Seasonality; BIO18 = Precipitation of Warmest Quarter; BIO19 = Precipitation of Coldest Quarter. The first two components explain 53.1% and 30.4% of the total variance, respectively.

| | Comp.1 | Comp.2 |
|---|---|---|
| bio1 | 0.806 | 0.140 |
| bio12 | 0.758 | -0.605 |
| bio14 | -0.360 | -0.878 |
| bio15 | 0.890 | 0.080 |
| bio18 | 0.790 | -0.544 |
| bio19 | -0.645 | -0.602 |
| Eigenvalues | 3.188 | 1.822 |
| Explained Variance | 53.135 | 30.360 |

**Table 2: Summary of MaxEnt model performance and settings for the eastern (E) and western (W) lineages (lin).** Regularization (Reg) refers to the multiplier applied to prevent model overfitting. Features indicate the types of feature classes used: l = linear, q = quadratic, h = hinge. nParameters is the number of model parameters. AICc.train and AICc.full represent the corrected Akaike Information Criterion values for the training extent and the full projection area, respectively. Training.AUC and Test.AUC refer to the area under the ROC curve for model evaluation on training and independent test datasets. Boyes refers to the Boyes index and TSS to the true skills statistics.

| lin | Regularization | Features | nParameters | AICc.train | AICc.full | Training.AUC | Test.AUC | Boyes | TSS |
|---|---|---|---|---|---|---|---|---|---|
| E | 0.5 | lq | 8 | 499.66 | 704.87 | 0.89 | 0.88 | 0.80 | 0.66 |
| W | 0.5 | lh | 5 | 249.76 | 332.42 | 0.85 | 0.83 | 0.75 | 0.67 |

774 **Figures and legends**

775

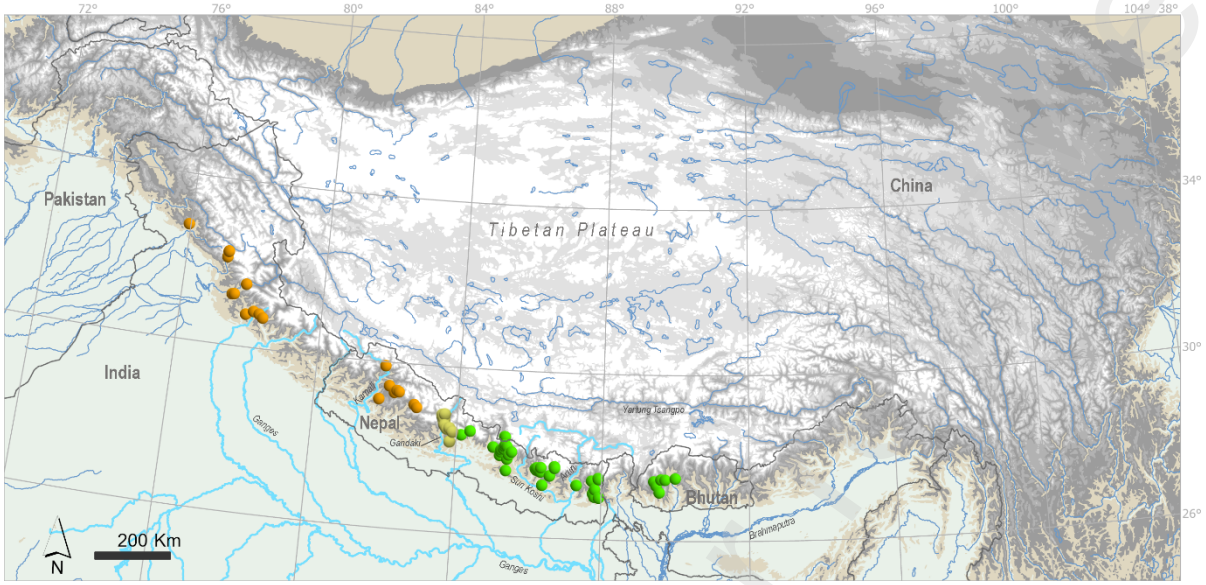


776

777 **Fig. 1–Distribution map of *Duttaphrynus himalaynus*.** Orange dots represent the western lineage

778 and green dots the eastern lineage, as identified in the present study, with the two separated by the

779 Kali Gandaki River valley. Yellow-green dots indicate records falling within the potential contact

780 zone between the lineages. The Ganges River and its major tributaries are shown in light blue. Map

781 was generated with ArcGIS Pro (ESRI).

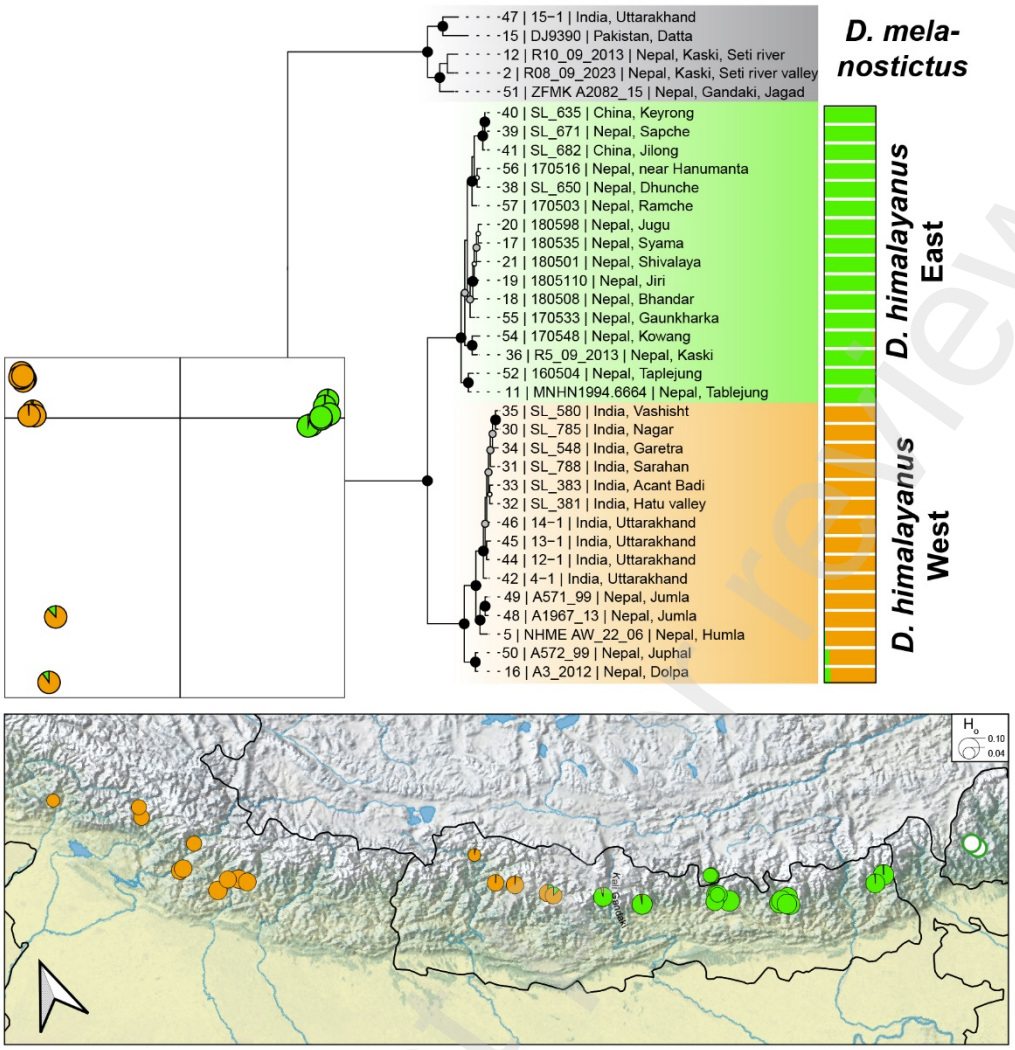


**Fig. 2– Phylogeny and genetic diversity of *Duttaphrynus himalayanus* based on nuclear markers.** The tree was obtained with IQ-TREE based on ~1.5 Mb and 36 samples, including *D. melanostictus* as outgroup. Barplots and pie charts show ancestry to two *D. himalayanus* clusters inferred by LEA, as also reported on the PCA, based on 5,744 SNPs. On the map, pie sizes are proportional to observed heterozygosity. On the tree, node circle size and colors represent branch support (large size, black: 100 %; middle size, grey: 95–99 %; small size, white: 70–94 %). Colors distinguish the two major lineages within *D. himalayanus* retrieved: the eastern lineage (*D. himalayanus* s. str., green) and the western lineage (*D.* cf. *himalayanus*, orange). The map also shows the two Bhutanese samples (white dots with green contour), analyzed separately and inferred as belonging to the eastern lineage with some divergence from the rest of the range (Fig. 4). Tree, barplots and PCA were visualized with Darjeeling custom R scripts; the map was generated using QGIS v3.24.

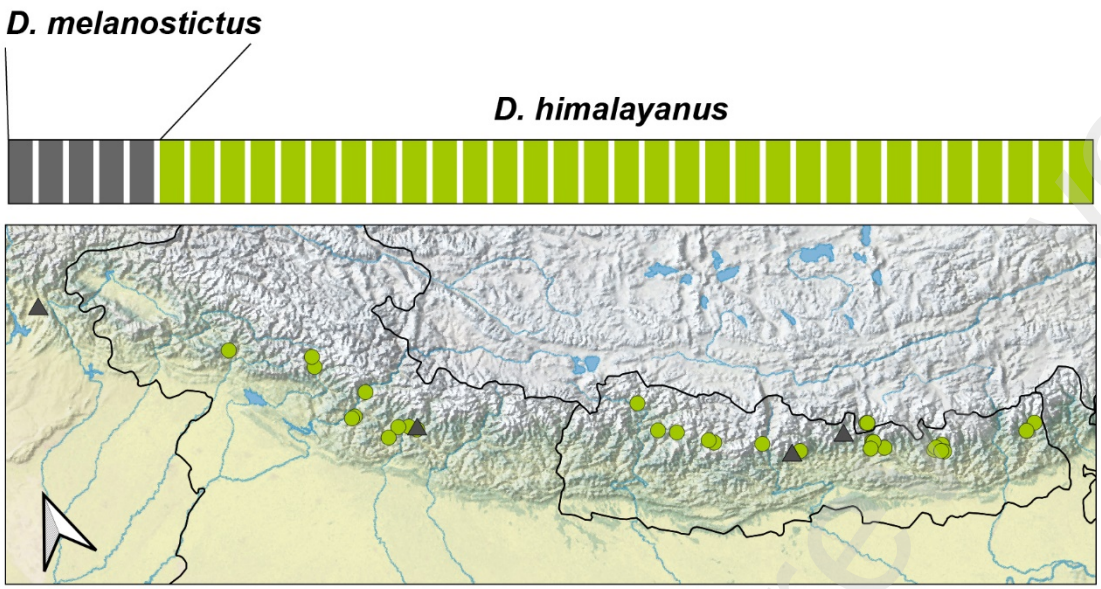


**Fig. 3–Assessment of interspecific gene flow between *Duttaphrynus himalayanus* and *D. melanostictus*.** Barplots (top) show individual ancestry proportions of our samples inferred by LEA (K = 2), based on 1,699 SNPs. The map shows the geographic origins of sampes. The analysis distinguishes *D. melanostictus* (grey, triangles on map) from *D. himalayanus* (olive green, circles on map) without a single instance of shared ancestry, indicating complete genetic isolation. Barplots were visualized with custom R scripts; the map was generated using QGIS v3.24.

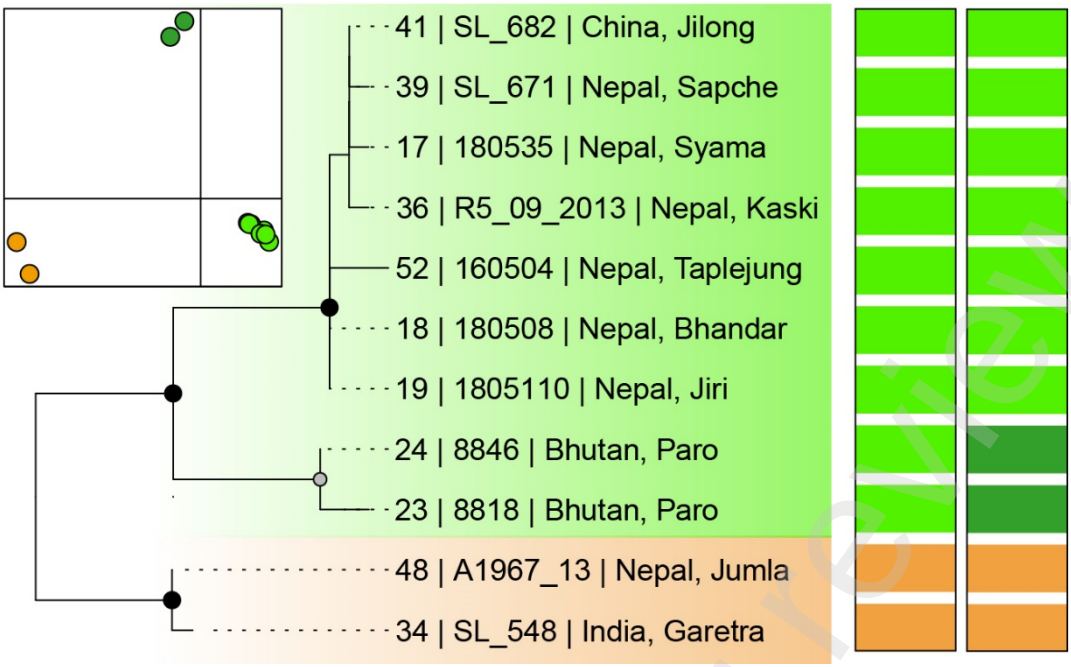


**Fig. 4– Genetic relationships of the low-quality Bhutan samples within the *Duttaphrynus himalayanus* diversity.** The tree was obtained with IQ-TREE based on ~6 kb and 11 samples (the two from Bhutan plus nine representative samples of the *D himalayanus* diversity). Barplots and pie charts show ancestry to two and three clusters inferred by LEA, as also reported on the PCA, based on 51 SNPs. On the tree, node circle size and colors represent branch support (large size, black: 100 %; middle size, grey: 95–99 %; small size, white: 70–94 %). Color shades on the tree distinguish the two major lineages within *D. himalayanus* (eastern lineage: green; western lineage: orange). The tree, barplots and PCA were visualized with custom R scripts.

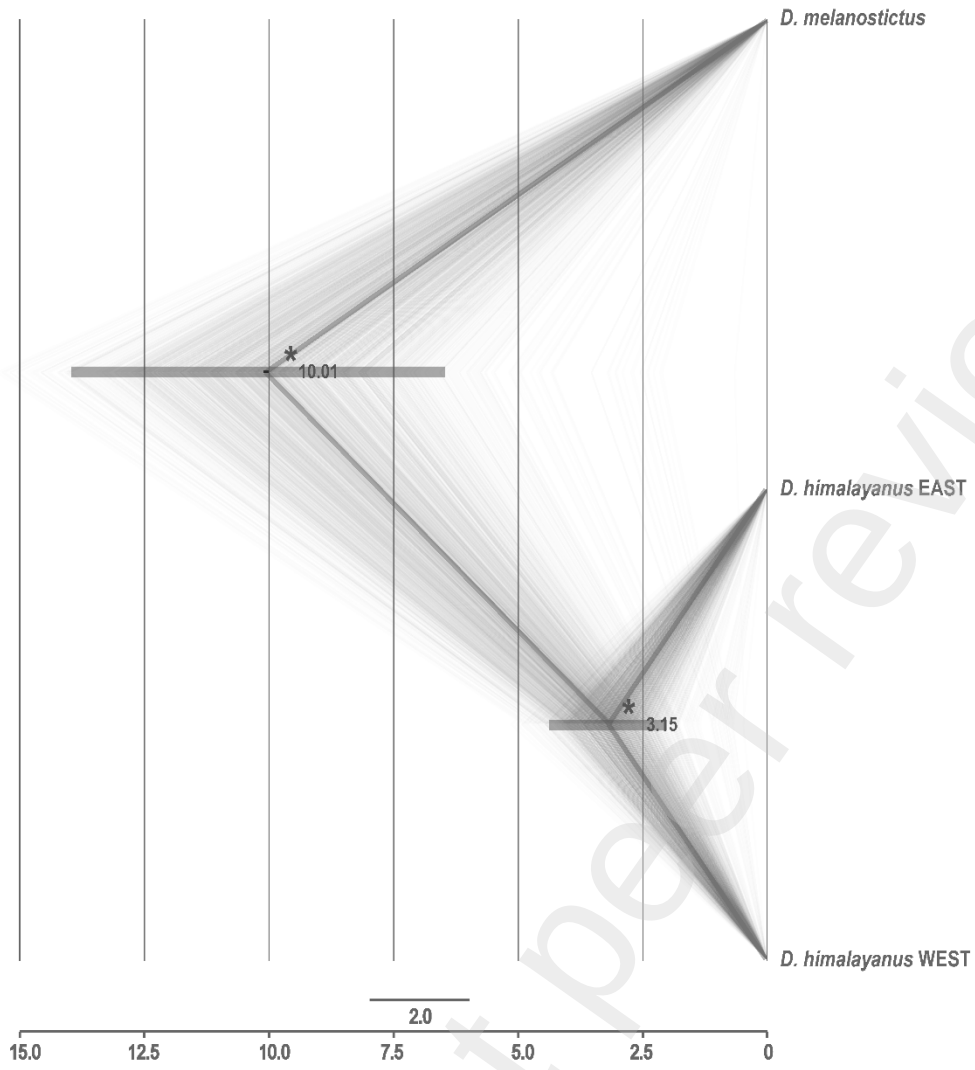


811

812 **Fig. 5–Time-calibrated species tree inferred using SNAPP based on ddRADseq data (13 *D.***

813 ***himalayanus* and two *D. melanostictus* samples; ~1.1 Mb).** The tree was visualized using

814 DensiTree. Node ages represent mean divergence time estimates; horizontal bars indicate 95% highest

815 posterior density (HPD) intervals. An asterisk indicates node support with posterior probability = 1.0.

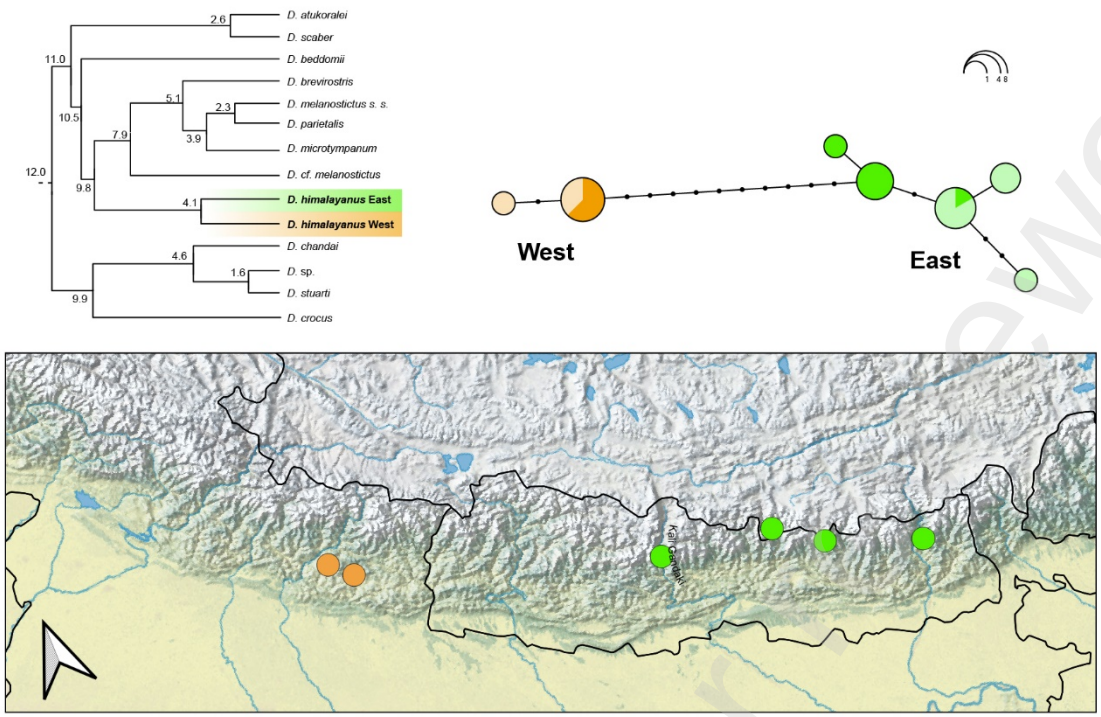


816

817 **Fig. 6– Mitochondrial phylogenetic placement and diversity of *Duttaphrynus himalayanus*.** The
818 time-calibrated phylogeny (top left) is based on partial mitogenomes [adapted from Dufresnes et al.
819 (2025)] and shows highlight the two major *D. himalayanus* lineages (western: orange; eastern: green).
820 The haplotype network (top right) is based on 23 published *D. himalayanus* sequences of the 16S
821 rRNA gene (compiled by (Dufresnes et al., 2025)); circle size is proportional to haplotype frequency,
822 colors correspond to the two identified lineages, with shades distinguishing georeferenced sequences
823 (plain colors) and sequences without locality information (faded colors). The map (bottom) shows the
824 geographic origin of geo-referenced 16S sequences, emphasizing the spatial segregation of the two
825 lineages east and west of the Kali Gandaki Valley.

826

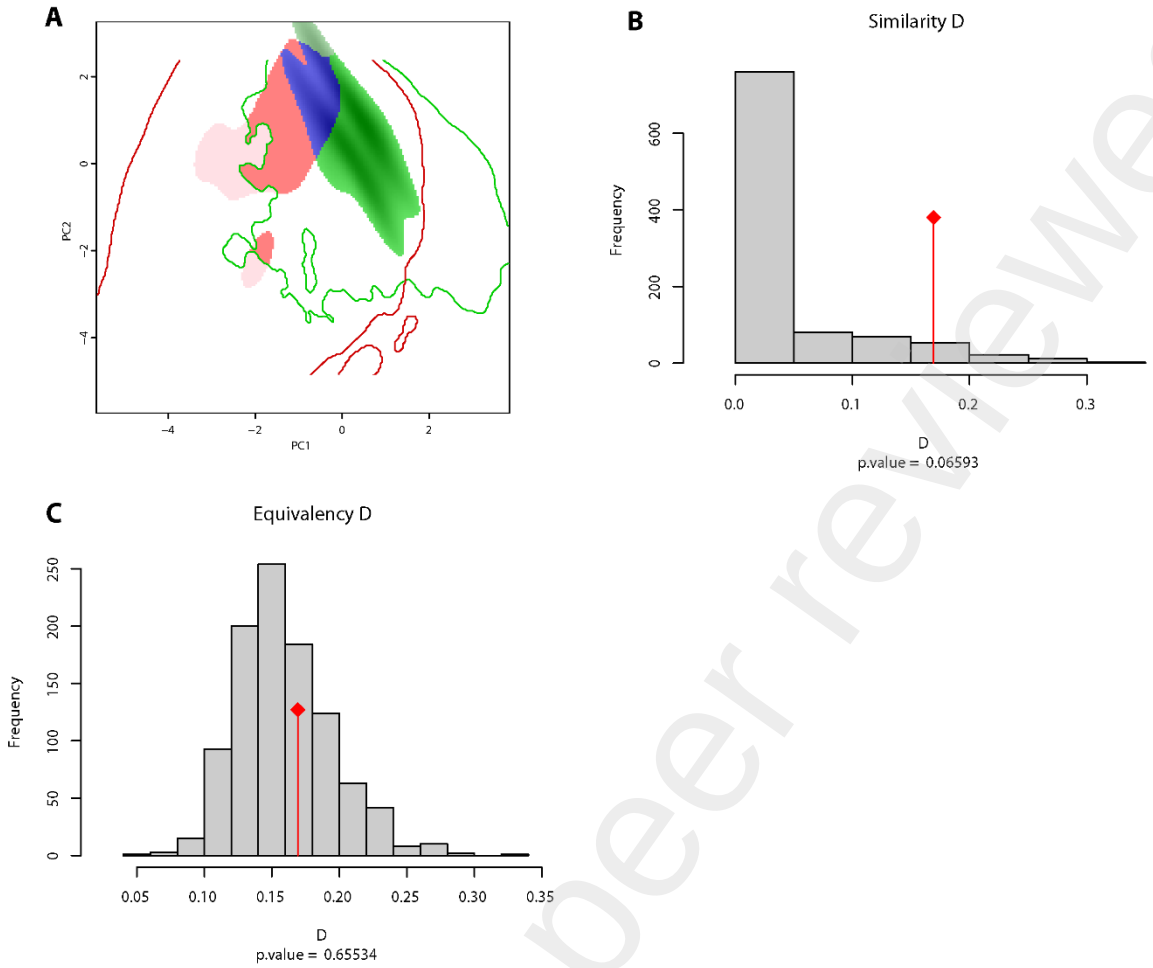


**Fig. 7–Niche overlap between the two lineages (East and West) of *Duttaphrynus himalayanus* in climate space. (A)** Climatic niche overlap analysis between the western and eastern lineage of *D. himalayanus*. The red solid line represents the potential climatic niche range available to the western lineage, while the green solid line denotes the potential climatic niche range of the easter lineage. Red areas denote the realized niche of the western clade, blue areas represent the niche overlap between both clades, and green areas indicate the realized niche of the eastern clade. **(B, C)** Histograms show the observed niche overlap (marked by red diamonds) and simulated overlaps (gray bars) derived from niche equivalency and similarity tests. Schoener's D index on the x-axis ranges from 0 (no overlap) to 1 (complete overlap). Significance levels ($p < 0.05$) indicate whether the observed overlap differs significantly from random expectations.

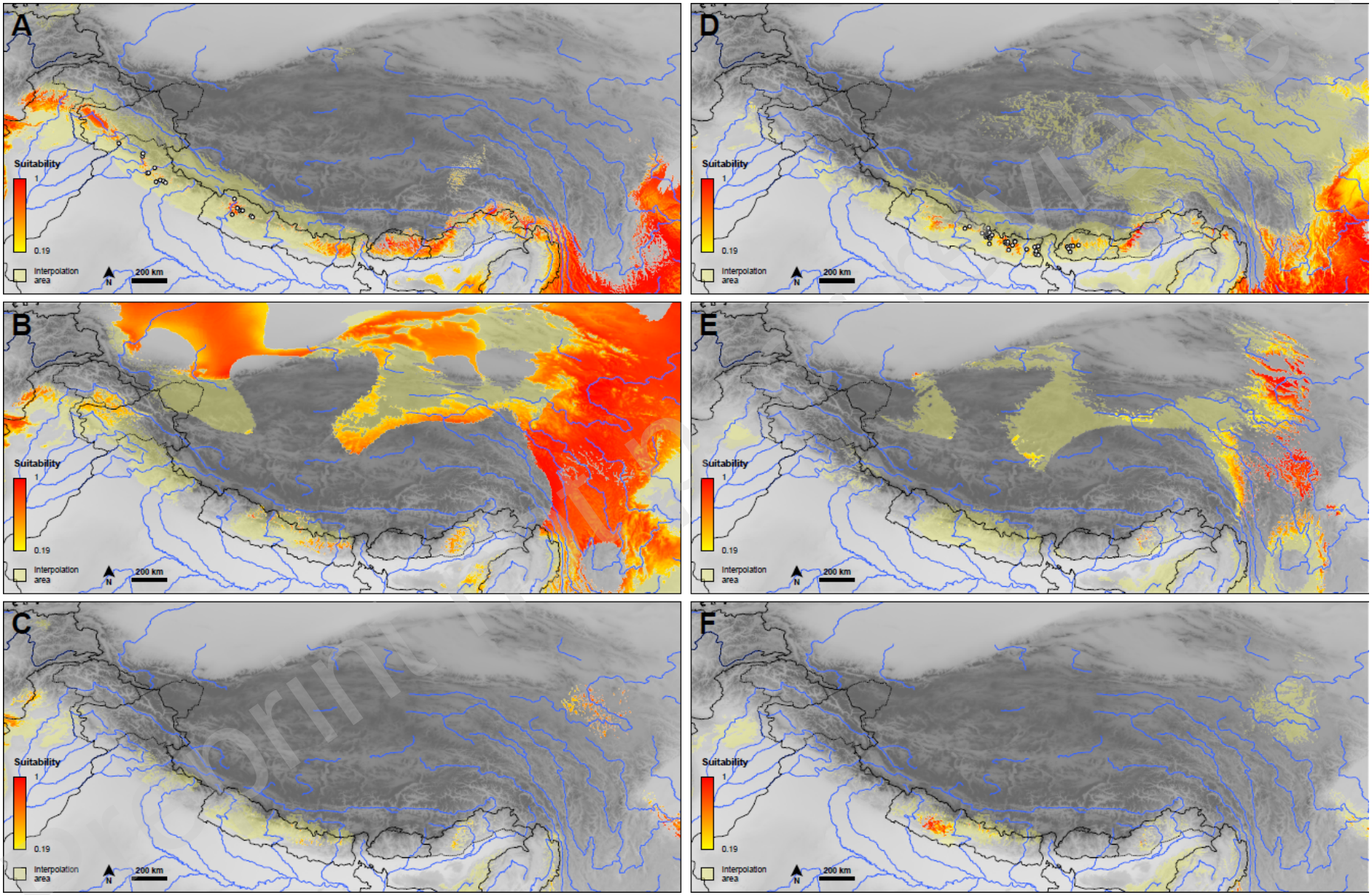

**Fig. 8–Present and hindcasted species distribution models (SDMs) for the western (A–C) and eastern (D–F) lineages of *Duttaphrynus himalayanus*, projected across three time periods: (A, D) present day, (B, E) the mid-Pliocene Warm Period (mPWP), and (C, F) the Marine Isotope Stage M2 cooling period.** The stretched color bar indicates habitat suitability, with increasing redness corresponding to higher suitability. Records of the respective lineage are indicated by circles in (A) and (D). The intrapolation area quantifies those areas which are within the training range of the models, i.e., have positive MESS scores.